

# **Correlation and co-localization of QTL for stomatal density and canopy temperature under drought stress in *Setaria***

Parthiban Thathapalli Prakash<sup>1,2,6</sup>, Darshi Banan<sup>2,3</sup>, Rachel E. Paul<sup>2,3</sup>, Maximilian J. Feldman<sup>4</sup>, Dan Xie<sup>2,3,7</sup>, Luke Freyfogle<sup>2,3</sup>, Ivan Baxter<sup>5</sup>, Andrew D.B. Leakey<sup>1,2,3</sup>

## **Affiliations:**

<sup>1</sup>Department of Crop Sciences, University of Illinois at Urbana-Champaign, Urbana, IL 61801, USA

<sup>2</sup>Institute for Genomic Biology, University of Illinois at Urbana-Champaign, Urbana, IL 61801, USA

<sup>3</sup>Department of Plant Biology, University of Illinois at Urbana-Champaign, Urbana, IL 61801, USA

<sup>4</sup>USDA-ARS, 24106 N Bunn Rd, Prosser, WA 99350, USA

<sup>5</sup>Donald Danforth Plant Science Center, 975 North Warson Road, St Louis, MO 63132, USA

## **Current affiliation**

<sup>6</sup>International Rice Research Institute, Los Baños, Philippines

<sup>7</sup>Department of Medicinal Chemistry and Molecular Pharmacology, Purdue University, West Lafayette, IN 47907, USA

Parthiban Thathapalli Prakash – [tpparthiban@gmail.com](mailto:tpparthiban@gmail.com)

Darshi Banan – [banan.darshi@gmail.com](mailto:banan.darshi@gmail.com)

Rachel E. Paul – [repaul9@gmail.com](mailto:repaul9@gmail.com)

Maximilian J. Feldman – [Max.Feldman@usda.gov](mailto:Max.Feldman@usda.gov)

Ivan Baxter – [IBaxter@danforthcenter.org](mailto:IBaxter@danforthcenter.org)

Dan Xie – [xie243@purdue.edu](mailto:xie243@purdue.edu)

Luke Freyfogle – [lukefreyfogle14@gmail.com](mailto:lukefreyfogle14@gmail.com)

Andrew D.B. Leakey – [leakey@illinois.edu](mailto:leakey@illinois.edu)

Number of tables – 2

Number of figures – 12

Word count – 3667

**Running title:** Physiological genetics of stomatal density and canopy temperature in setaria

# **Highlight**

This article reports a phenotypic and genetic relationship between two water use related traits operating at leaf level and canopy level in a C<sub>4</sub> model crop species.

# **Abstract**

Mechanistic modeling indicates that stomatal conductance could be reduced to improve water use efficiency (WUE) in C<sub>4</sub> crops. Genetic variation in stomatal density and canopy temperature was evaluated in the model C<sub>4</sub> genus, *Setaria*. Recombinant inbred lines (RIL) derived from a *Setaria italica* x *Setaria viridis* cross were grown with ample or limiting water supply under field conditions in Illinois. An optical profilometer was used to rapidly assess stomatal patterning and canopy temperature was measured using infrared imaging. Stomatal density and canopy temperature were positively correlated but both were negatively correlated with total above-ground biomass. These trait relationships suggest a likely interaction between stomatal density and the other drivers of water use such as stomatal size and aperture. Multiple QTLs were identified for stomatal density and canopy temperature, including co-located QTLs on chromosomes 5 and 9. The direction of the additive effect of these QTLs on chromosome 5 and 9 were in accordance with the positive phenotypic relationship between these two traits. This suggests a common genetic architecture between stomatal patterning in the greenhouse and canopy transpiration in the field, while highlighting the potential of setaria as a model to understand the physiology and genetics of WUE in C<sub>4</sub> species.

**Keywords:** *Setaria*, stomata, canopy temperature, drought, quantitative trait loci, optical tomography.

## Introduction

Drought stress is the primary limiting factor to crop production worldwide (Boyer, 1982). This is underpinned by the unavoidable loss of water vapor from leaves, via stomata, to the atmosphere in order for CO<sub>2</sub> to move in the reverse direction and be assimilated through photosynthesis. In the coming decades, crops are likely to experience increasingly erratic rainfall patterns, with more frequent and intense droughts, due to climate change (Stocker *et al.*, 2013). Irrigation of crops already accounts for ~70% of freshwater use, limiting the sustainability of any increase in irrigation to address drought limitations (Hamdy *et al.*, 2003). Consequently, there is great interest in understanding and improving crop water-use efficiency (WUE; Leahey *et al.*, 2019) as well as crop drought resistance (Cattivelli *et al.*, 2008).

Substantial advances have been made in understanding WUE and drought resistance at the genetic, molecular, biochemical and physiological levels in the model species, *Arabidopsis thaliana* (Zhang *et al.*, 2004; Valliyodan and Nguyen, 2006; Nakashima *et al.*, 2012). Unfortunately, efforts to translate this knowledge into improved performance of crop plants in the production environment have not resulted in success as frequently as hoped (e.g. Nelson *et al.*, 2007; Nemali *et al.*, 2015). Physiological, agronomic and breeding studies directly in crops have also resulted in improved drought avoidance and drought tolerance (e.g. Condon *et al.*, 2004; Sinclair *et al.*, 2017), but there are challenges associated with trying to apply modern systems biology and bioengineering tools to crops that are relatively large in stature and have generation times of several months. Consequently, *Setaria viridis* (L.) has been proposed as a model C<sub>4</sub> grass that has characteristics that make it tractable for systems and synthetic biology while also being closely related to key C<sub>4</sub> crops, so that discoveries are more likely to translate to production crops (Brutnell *et al.*, 2010; Li and Brutnell, 2011). This study aimed to assess natural genetic variation in *Setaria* for two key traits related to WUE and drought response: stomatal density and canopy temperature (as a proxy for the rate of whole-plant water use).

*Setaria italica* and *Setaria viridis* are model C<sub>4</sub> grasses belonging to the panicoideae subfamily, which also includes maize, sorghum, sugarcane, miscanthus and switchgrass (Brutnell *et al.*, 2010; Li and Brutnell, 2011). Foxtail millet (*Setaria italica*) is also a food crop in

China and India (Devos *et al.*, 1998). The availability of sequence data for its relatively small diploid ( $2n = 18$ ) genome, short life cycle, small stature, high seed production, and amenability for transformation makes *Setaria* a good model species for genetic engineering (Brutnell *et al.*, 2010; Bennetzen *et al.*, 2012). In addition, *Setaria* is adapted to arid conditions and is a potential source of genes conferring WUE and drought resistance.

Whole plant WUE is the ratio of plant biomass accumulated to the amount of water used over the growing season (Condon *et al.*, 2004; Morison *et al.*, 2007; Blum, 2009; Tardieu, 2013). WUE at the leaf level is a complex trait controlled by factors including photosynthetic metabolism, stomatal characteristics, mesophyll conductance and hydraulics (Farquhar *et al.*, 1989; Condon *et al.*, 2002; Hetherington and Woodward, 2003). At the whole-plant scale it is modified by canopy architecture and root structure and function (Martre *et al.*, 2001; White and Snow, 2012).

Stomata regulate the exchange of water and carbon dioxide ( $\text{CO}_2$ ) between the internal leaf airspace and the atmosphere (Hetherington and Woodward, 2003; Bertolino *et al.*, 2019). Stomatal conductance ( $g_s$ ), which is the inverse of the resistance to  $\text{CO}_2$  uptake and water loss, is controlled by a combination of stomatal density, patterning across the leaf surface, maximum pore size, and operating aperture (Faralli *et al.*, 2019; Nunes *et al.*, 2020). Of these traits, stomatal density is most simple to measure (Dow and Bergmann, 2014). Consequently, genetic variation in stomatal density has been explored in a range of species, including the identification of quantitative trait loci (QTL) in rice (Laza *et al.*, 2010), wheat (Schoppach *et al.*, 2016; Shahinnia *et al.*, 2016), barley (Liu *et al.*, 2017), *Arabidopsis* (Dittberner *et al.*, 2018; Delgado *et al.*, 2019), brassica (Hall *et al.*, 2005), poplar (Dillen *et al.*, 2008) and oak (Gailing *et al.*, 2008). However, there is a notable knowledge gap regarding genetic variation in stomatal density within  $C_4$  species. While many genes involved in the regulation of stomatal development are known in *Arabidopsis*, investigation of whether their orthologs retain the same function in grasses and other phylogenetic groups that include the major crops is still relatively nascent (e.g. Raissig *et al.*, 2017; Lu *et al.*, 2019; Mohammed *et al.*, 2019). This is in part because standard protocols for measuring stomatal density are still laborious and time consuming, which slows the application of quantitative, forward, and reverse genetics

approaches to identifying candidate genes and confirming their function. Therefore, improved methods for acquiring and analyzing images of stomatal guard cell complexes and other cell types in the epidermis are an area of active research (Haus *et al.*, 2015; Dittberner *et al.*, 2018; Fetter *et al.*, 2019; Li *et al.*, 2019). In addition, alternative approaches to rapidly screen stomatal conductance or rates of transpiration at the leaf and canopy scales (including temperature as a proxy) have also been developed and used to reveal genetic variation in traits related to drought stress and WUE (Liu *et al.*, 2011; Bennett *et al.*, 2012; Awika *et al.*, 2017; Prado *et al.*, 2018; Deery *et al.*, 2019; Violet-Chabrand and Lawson, 2019). However, the expected links between genetic variation in stomatal density and measures of water use, which would be expected in theory, are rarely tested and when tested, the results are inconsistent (e.g. Fischer *et al.*, 1998; Ohsumi *et al.*, 2007; Kholová *et al.*, 2010; Schoppach *et al.*, 2016).

To address these questions, we used a field study of a biparental mapping population developed from an interspecific cross between *Setaria viridis* (A10) and *Setaria italica* (B100).

The study was designed with the aim of (i) applying rapid, image-based methods for phenotyping stomatal density and canopy water use; (ii) Identifying variation in stomatal patterning, canopy temperature and productivity; (iii) assessing trait relationships between stomatal density, canopy temperature and biomass production; and (iv) identifying quantitative trait loci for these traits in *Setaria*, grown in the field under wet and dry treatments.

## Materials and methods

### *Plant material*

This study used a population of 120 F<sub>7</sub> recombinant inbred lines (RIL), which were generated by an interspecific cross between domesticated *Setaria italica* accession B100 and a wild-type *Setaria viridis* accession A10 (Devos *et al.*, 1998; Wang *et al.*, 1998).

### *Greenhouse experiment*

Variation in stomatal density among the RILs was assessed in a greenhouse study at the University of Illinois, Urbana Champaign in 2015. Plants were grown in pots (10 x 10 x 8.75 cm) filled with potting mixture (Metro-Mix 360 plus, Sun Gro Horticulture). Three seeds were sown

directly into the pot. After germination, plants were thinned to one plant per pot. Growth conditions were 30/24 °C during the day/night and plants received supplemental photosynthetically active radiation from high-pressure sodium and metal halide lamps during the day (350  $\mu\text{mol m}^{-2} \text{s}^{-1}$  on a 16-h day / 8-h night cycle). Throughout the growing period, water was added to pot capacity along with fertilizer (EXCEL-CAL-MAG 15-5-5) 2-3 times a week.

The youngest fully expanded leaf was excised from the plant 17 - 22 days after sowing, covered in wet paper towel, sealed in airtight bags, and stored at 4°C. Within 48 hours, a sample was excised with a razor blade from midway along the leaf to provide a cross-section from one leaf margin to the midrib (approximately 20-30 mm length, 3- 20 mm wide). This sample was attached to a glass microscope slide using double-sided adhesive tape and the abaxial surface immediately imaged using an  $\mu\text{surf}$  explorer optical topometer (Nanofocus, Oberhausen, Germany (Haus *et al.*, 2015)). Four fields of view in a transect from the midrib to the edge of a single leaf were imaged using a 20x magnification objective lens. The images were then exported into TIF files and the stomatal number was counted using the cell counter tool in ImageJ software (<http://rsbweb.nih.gov/ij/>). Stomatal density was calculated by normalizing the number of stomata with the area of the field of view (0.64  $\text{mm}^2$ ). Data from each of the four fields of view were treated as subsamples and averaged to estimate mean stomatal density for each replicate plant of a given RIL.

### *Field experiment*

The field experiment to assess variation in canopy temperature and total above-ground biomass was conducted at the SoyFACE field site, University of Illinois, Urbana Champaign in 2015, in the manner described by Feldman *et al.* (2017). The average air temperature over the growing season was 21.5 °C with a relative humidity of 82 % (Figure 1). In brief, plants were germinated in plug trays in the greenhouse and then after 9 days after sowing, seedlings were hand transplanted (July 15, 2015) into plots at the field site. Twelve retractable awnings (Gray *et al.*, 2016) were placed over the plots to block all water from any rainfall event in both wet and dry treatments. Drip irrigation was supplied once a week in order to maintain greater soil moisture in the wet treatment.

Each genotype subplot in the experiment measured 25 by 20 cm and contained 30 plants with a grid spacing of 5 cm between the plants. There was 25 cm space for the alleyway between two columns of plots and 10 cm spacing between the rows of plots. Each awning contained 66 subplots including six check plots of the B100 accession. The volumetric water content in the center of each awning was measured every 15 minutes throughout the growing season using soil moisture probes (CS650; Campbell Scientific) at 5 and 25 cm depths.

Canopy temperature of all field plots under both wet and dry treatments was measured 30 and 32 days after sowing (DAS) once canopy closure had occurred in all plots. A telescopic boom lift was used to collect images from a height of 9.1 m above the ground using a handheld infra-red camera (FLIR T400, FLIR Systems, Boston, MA, USA). On each date, one infrared and one RGB image was acquired for each awning, which consisted of 66 plots (Figure 2). The time of the measurements was between 11 am and 3 pm. Infrared imaging was performed only during clear and sunny weather conditions. Data from the 36 pixels at the center of each genotype subplot was used to estimate the canopy temperature (FLIR Tools, FLIR Systems, Boston, MA, USA). This ensured that temperature data were only sampled from pixels completely covered by plant canopy and not containing data from soil in the nearby alleys between plots.

Three plants from the center of each plot were destructively harvested 30 days after panicle emergence to estimate the shoot biomass. The plants were cut at the base and the leaf, stem and the panicles were separated and dried at 65°C. The dried weights of leaf, stem and panicle were summed to obtain the total shoot biomass.

### *Data analysis*

The greenhouse experiment was conducted with four replicates of each RIL arranged in a randomized complete block design with 120 genotypes as described in the equation below, where  $Y_{ij}$  is the individual observation of the trait of interest,  $\mu$  is the overall mean, Genotype  $i$  is the effect of the  $i^{\text{th}}$  genotype, Block  $j$  is the effect of the  $j^{\text{th}}$  block and  $\epsilon_{ij}$  is the error term.

$$Y_{ij} = \mu + \text{Genotype}_i + \text{Block}_j + \varepsilon_{ij}$$

The field experiment was conducted as a randomized complete block design in a split plot arrangement with 3 blocks, 2 treatment conditions, 12 awnings nested within treatments and blocks and 120 genotypes as described below

$$Y_{ijkl} = \mu + \text{Block}_i + \text{Treatment}_j + \varepsilon_{ij} + \text{Awning}_{k(ij)} + \text{Genotype}_l + \text{Genotype} * \text{Treatment}_{lj} + \varepsilon_{ijkl}$$

where  $Y_{ijkl}$  is the individual observation of the trait of interest,  $\mu$  is the overall mean,  $\text{Block}_i$  is the effect of the  $i^{\text{th}}$  block,  $\text{Treatment}_j$  is the effect of the  $j^{\text{th}}$  treatment and  $\varepsilon_{ij}$  is the first error term,  $\text{Awning}_{k(ij)}$  is the  $k^{\text{th}}$  awning nested within  $\text{Block}_i$  and  $\text{Treatment}_j$ ,  $\text{Genotype}_l$  is the  $l^{\text{th}}$  genotype,  $\text{Genotype} * \text{Treatment}_{lj}$  is the interaction between  $\text{Genotype}_l$  and  $\text{Treatment}_j$  and  $\varepsilon_{ijkl}$  is the second error term.

The broad sense heritability on a line mean basis was computed using the variance components from the mixed model using the below formula.

$$H^2_{\text{broad sense}} = \frac{\sigma^2_{(\text{Genotype})}}{\sigma^2_{(\text{Genotype})} + \frac{\sigma^2_{(\text{Genotype} \times \text{Treatment})}}{n_{\text{treatments}}} + \frac{\sigma^2_{(\text{residual})}}{n_{\text{reps}}}}$$

The variance components from the mixed model were extracted using lme4 package in R (Bates *et al.*, 2015). Best linear unbiased predictors (BLUPs) were calculated for each trait of interest using the experimental designs discussed earlier where genotypes and blocks were considered as random effects and treatment and awning as fixed effects.

The quantitative trait loci (QTL) mapping was performed on the BLUP values for stomatal density and canopy temperature under different treatments and sampling dates using ~1400 Single Nucleotide Polymorphism (SNP) markers. Mapping was performed using a custom biparental linkage mapping program (Feldman *et al.*, 2017) based upon the functionality

encoded within the R/qtl (Broman *et al.*, 2003) and funqtl (Kwak *et al.*, 2014) packages in R. A two-step procedure was performed (Feldman *et al.*, 2017). First a single QTL model genome scan was performed using Haley-Knott regression to identify QTLs with LOD score higher than the significant threshold obtained through 1000 permutations at alpha 0.05. Second a stepwise forward/backward selection procedure was performed to identify an additive, multiple QTL model based upon maximization of penalized LOD score. The two-step procedure was conducted on all the traits and timepoints. QTLs that lie within 20 cM window are considered to be the same QTL.

## Results

### *Soil moisture profile*

Soil moisture content was equivalent in the wet and dry treatments at the beginning of the experiment (Figure 3). As time progressed, plants in the wet treatment continued to have adequate water supply (30 – 40 % vol/vol) throughout the growing period. By contrast, plants in the dry treatment experienced progressively drier soil conditions as the water they transpired was not replaced by rainfall or irrigation. The soil moisture was reduced in the dry treatment compared to the wet treatment at 5 cm and 25 cm depth by 20 DAS, resulting in a statistically significant interaction between treatment and time ( $p < 0.001$ ) as well as significant overall effects of drought treatment ( $p < 0.001$ ), depth ( $p < 0.001$ ) and time ( $p < 0.001$ ). Midday canopy temperature data was collected after this date, 30 and 32 DAS, when plants in the dry treatment were experiencing rapidly decreasing availability of soil moisture. This indicates that while plants in the dry treatment were subjected to limited water supply, they were still physiologically active i.e. drought stress was moderate.

### *Genotypic variation in stomatal density and canopy temperature*

Among the 120 RILs, stomatal density on the abaxial surface of the youngest fully expanded leaf ranged between 58 to 115 stomata/mm<sup>2</sup> with a mean of 84 stomata/mm<sup>2</sup> (Figure 4 and Figure 5). The broad sense heritability of stomatal density was 0.58. Among the 120 RILs, the mean canopy temperature at midday ranged from 28.8- 31.9 °C at 30 DAS and

28.6- 31.9 °C at 32 DAS in the wet treatment, and from 30.9- 39.2 °C at 30 DAS and 29.3- 38.1 °C at 32 DAS in the dry treatment. The mean midday canopy temperature across the RIL population was greater in the dry treatment than the wet treatment at both 30 DAS (32.9 °C versus 29.9 °C;  $p < 0.001$ ) and 32 DAS (32.0 °C versus 29.6 °C;  $p < 0.001$ ; Figure 6), with the treatment effect being slightly greater at 30 DAS (3.0 °C) than 32 DAS (2.4 °C). Midday canopy temperature was positively correlated between the two measurement dates for both wet ( $\rho = 0.78$ ,  $p < 0.001$ ) and dry ( $\rho = 0.66$ ,  $p < 0.001$ ) conditions, which gives confidence in the phenotyping method (Figure 7). The broad sense heritability of canopy temperature was 0.54 and 0.40 in 30 and 32 DAS, respectively.

#### *Phenotypic relationships among canopy temperature, stomatal density and total biomass*

Midday canopy temperature was negatively correlated with total above-ground biomass under both wet and dry treatments at both 30 DAS (wet:  $r = -0.38$ ,  $p < 0.001$ ; dry:  $r = -0.32$ ,  $p < 0.001$ ) and 32 DAS (wet:  $r = -0.49$ ,  $p < 0.001$ ; dry:  $r = -0.46$ ,  $p < 0.001$ ; Figure 8). The average increase in total above-ground biomass production associated with a decrease in midday canopy temperature of 1 °C was greater in the wet treatment than the dry treatment on both measurement dates (Table 1). The amount of variation in total above-ground biomass production explained by variation in midday canopy temperature was slightly greater in the wet treatment than the dry treatment on both sampling dates (Table 1). The parental line A10 recorded was one of the genotypes with lowest biomass and highest canopy temperature under both treatments and days of measurement, while the parental line B100 had trait values that were close to the mean of the population.

Stomatal density was positively correlated with midday canopy temperature under both wet and dry treatments at both 30 DAS (wet:  $r = 0.40$ ,  $p < 0.001$ ; dry:  $r = 0.38$ ,  $p < 0.001$ ) and 32 DAS (wet:  $r = 0.37$ ,  $p < 0.001$ ; dry:  $r = 0.39$ ,  $p < 0.001$ ; Figure 9). And, correspondingly, stomatal density was negatively correlated with total above-ground biomass under both dry ( $r = -0.33$ ,  $p < 0.001$ ) and wet ( $r = -0.23$ ,  $p = 0.012$ ) conditions (Figure 10). The correlation between stomatal density and total biomass was stronger under the dry treatment than the wet treatment.

## QTL mapping results

QTL analysis identified three significant loci for stomatal density and eight significant loci for canopy temperature (Table 2, Figure 11). The proportion of phenotypic variation associated with these QTLs ranged between 8 to 23 percent for both the traits. QTLs across different traits were considered to be overlapping if they were within a 20cM window and others that fall outside this window were considered to be unique QTLs (Feldman *et al.*, 2017). Two QTLs co-localized for both stomatal density and canopy temperature one on chromosome 5 and one on chromosome 9. All four alleles had negative additive effects, indicating that the B100 allele was reducing both stomatal density and canopy temperature.

## Discussion

This study successfully characterized phenotypic and genetic variation in stomatal density and rates of canopy water use in *Setaria*, which can be used as a foundation for future studies to apply systems biology approaches to advance understanding of WUE and drought resistance in *C<sub>4</sub>* species. Significant trait correlations were detected among stomatal density, canopy temperature and total above-ground biomass both in the wet and dry treatments.

The stomatal densities of RILs in this population (58 – 115 mm<sup>-2</sup>) were slightly greater than previously reported for faba bean (30 – 75 mm<sup>-2</sup> Khazaei *et al.*, 2014) and wheat (36 – 92 mm<sup>-2</sup> Schoppach *et al.*, 2016; 43 – 92 mm<sup>-2</sup> Shahinnia *et al.*, 2016), but generally lower than *Arabidopsis* (90 – 210 mm<sup>-2</sup> Dittberner *et al.*, 2018) and rice (273 – 697 mm<sup>-2</sup> Laza *et al.*, 2010; 200 – 400 mm<sup>-2</sup> Kulya *et al.*, 2018). While the magnitude of variation in stomatal density among the RIL population was sufficient to allow for QTL mapping and analysis of trait correlations, the parents of the population were not selected on the basis of this trait. Thus, the resulting magnitude of variation across the population was relatively modest. It would be valuable to investigate how much more variation for stomatal density may be found among genotypes within either *S. italica* or *S. viridis*, as well as the genus as a whole. The present study provided a proof of concept for the use of optical tomography to image the leaf epidermis. As proposed by Haus *et al.* (2015), optical tomography does not require sample preparation steps and can also

be used on frozen leaf samples. This was significantly less laborious and more convenient than standard methods of taking leaf imprints of fresh leaves with dental gum and nail varnish (Rowland-Bamford *et al.*, 1990).

The magnitude of variation in canopy temperature across the *Setaria* RIL population was similar to that observed for sorghum (Awika *et al.*, 2017) and wheat (Mason *et al.*, 2013) RIL populations. Variation in canopy temperature among the RIL population were similar on 30 DAS (wet 3.1 °C, dry 8.3 °C) and 32 DAS (wet 3.3 °C, dry 8.8 °C) and canopy temperature was correlated across the two dates sampled for both the wet ( $\rho = 0.78$ ) and dry treatments ( $\rho = 0.66$ ). This might be considered surprising given the highly dynamic nature of canopy temperature in response to wind gusts, diurnal variation in solar radiation, and daily or seasonal variation in climate. But, the reproducibility of the data across dates is consistent with the comprehensive analysis by Deery *et al.* (2019), which analyzed 98 independent timepoints of canopy temperature data collected for a wheat population over 14 dates in two years. They concluded that canopy temperature could be reliably screened from one or two sampling points if data was collected under clear sky conditions in the afternoon, as was done in the current study. The present study also highlighted that *Setaria* as a highly tractable model for field trials because its small stature allows non-destructive, remote-sensing approaches to phenotyping, such as thermal imaging, to be performed on hundreds of replicated plots using hand-held cameras and a boom lift. This is significantly simpler in terms of data acquisition and data analysis than using drones or vehicles to gather data across field trials of crops with larger stature that require field trials covering larger areas (Deery *et al.*, 2016; Sagan *et al.*, 2019).

Canopy temperature was negatively correlated with the total above-ground biomass of the *Setaria* RILs under both wet and dry conditions. This is consistent with RILs that had higher temperatures due to less evaporative cooling being able to assimilate less CO<sub>2</sub>, and therefore producing less biomass, which was expected based on theory and previous studies (Fischer *et al.*, 1998; Jones, 2004). In addition, canopy temperature was significantly greater in the dry treatment compared to the wet treatment, which was consistent with stomatal closure reducing water use and evaporative cooling when there is limited water availability (Turner *et al.*, 2001). The relationship between canopy temperature and biomass was stronger in the wet

treatment than the dry treatment on both measurement dates. This was reflected in canopy temperature explaining a greater proportion of variation in biomass (i.e. greater correlation coefficient) and a greater loss of biomass production per unit increase in canopy temperature under wet than dry conditions. This pattern of response is also consistent with prior observations (Bennett *et al.*, 2012; Mason *et al.*, 2013), but does not appear to have been the subject of much discussion. While it may seem initially counterintuitive that the relationship between the rate of water use and productivity would be weaker when water is limiting, it is consistent with genotypes that have inherently high rates of transpiration (i.e. cooler canopies) having greater reductions in productivity in response to drought stress than genotypes with inherently low rates of transpiration (i.e. warmer canopies). We suggest that this differential response may be conserved. And, it adds weight to the argument that genetic variation in WUE is best screened under well-watered conditions (Leakey *et al.*, 2019).

The positive correlation of stomatal density with the canopy temperature under drought stress suggests that the relationship between these two traits is complicated, since – if all else is equal – greater stomatal density would be expected to increase transpiration and lead to canopy cooling. Consistent with that theory, previous studies have reported that stomatal density is positively correlated with WUE (Xu and Zhou, 2008). However stomatal conductance is influenced by multiple factors, including stomatal density, maximum size and operating aperture (Dow and Bergmann, 2014; Faralli *et al.*, 2019). This implies that greater stomatal density within this population of *Setaria* RILs was associated with a developmental or functional shift that led to smaller stomatal apertures and lower rates of transpiration. As a result, within this population, lower stomatal density was also associated with greater biomass production. But, it should be noted that this relationship may be a function of the forced recombination across many parental alleles that is found in a RIL population. Breaking up gene linkage that can result from selection has been proposed to be a powerful approach to understand the biophysical basis for phenotypic relationships (Des Marais *et al.*, 2013). The observed positive correlation may reflect the developmental trade-off where stomatal size and stomatal density are widely found to be negatively correlated due to a limited amount of space on the epidermis (Shahinnia *et al.*, 2016; Faralli *et al.*, 2019), but this needs to be confirmed experimentally. By

contrast, stomatal density was either not correlated or weakly, positively correlated with yield in wheat grown under both well-watered and drought treatments (Khazaie *et al.*, 2011; Schoppach *et al.*, 2016; Shahinnia *et al.*, 2016; Faralli *et al.*, 2019). So, the balance of trade-offs between stomatal density and aperture may be different among different biparental mapping populations, if not more generally in *Setaria* versus wheat. It would be valuable to compare if the same phenotypic relationship is observed across other biparental populations within these species as well as across natural accessions of these crops.

This study identified three unique QTL each for stomatal density and canopy temperature. All three of the canopy temperature QTL were robust in terms of being observed in both the wet and dry treatments. In addition, the canopy temperature QTLs on chromosomes 5 and 9 co-localized with QTLs for stomatal density (Figure 11). Genetic fine mapping would be required to discount the possibility that there are two loci in linkage at those locations. But, the observed pattern could be the result of pleiotropy, where a single locus regulates both traits. And, this would be consistent with the consistent direction of the allelic effects as well as positive correlation between the two traits, as well as the theoretical expectation that stomatal patterning on the epidermis influences transpiration rates. In that case, the ability to detect the same QTL in a greenhouse screen of stomatal density as for canopy temperature in the field suggests that rapid controlled environment screening might be a tractable way to accelerate progress in understanding and manipulating epidermal patterning and WUE in *Setaria*. The small stature of *Setaria* makes it particularly amenable for that approach. More broadly, the proportion of phenotypic variation explained by the stomatal density QTLs in *Setaria* were also similar to those of faba bean (Khazaei *et al.*, 2014), rice (Laza *et al.*, 2010), and wheat (Shahinnia *et al.*, 2016; Wang *et al.*, 2016).

Previous studies have identified many QTLs for different morphological and physiological traits using the same RIL population in *Setaria* in both controlled environment and field experiments (Mauro-Herrera and Doust, 2016; Feldman *et al.*, 2017; Banan *et al.*, 2018; Feldman *et al.*, 2018; Ellsworth *et al.*, 2020). These include measurements of traits with direct relevance to this study such as WUE of biomass production (i.e. biomass production relative to water use, as assessed by image analysis and metered irrigation on a high-throughput

phenotyping platform linked to a controlled environment chamber). Meta-analysis of all the studies (Figure 12) reveals that QTL for stomatal density and canopy temperature overlap with QTLs for WUE,  $\delta^{13}\text{C}$  (Ellsworth *et al.*, 2020), plant height, panicle emergence, and various measures of above-ground productivity (Feldman *et al.*, 2017; Banan *et al.*, 2018) on chromosomes 5, 7 and 9. It is noteworthy that the percentage of the phenotypic variance explained by these QTLs for stomatal density and canopy temperature was typically equal to, or greater than, for the other traits assessed to date. One explanation for this would be that these loci directly regulate traits related to stomatal function and then indirectly influence the other traits via effects on crop water use. There is no reason to think the experimental design used here result in any greater statistical power to detect genotype to phenotype associations than the other studies. However, additional experimentation where all traits are measured simultaneously is needed to test this notion definitively.

In conclusion, this study identified genetic loci in *Setaria* that are associated with variation in stomatal density as well as many other traits important to WUE, productivity and drought resistance. This suggests that *Setaria* is an experimentally tractable model system that would be highly suitable for more in-depth investigation of the mechanisms underpinning stomatal development and their influence on WUE in  $\text{C}_4$  species. An additional benefit to identifying QTLs and genes in *Setaria* is that it is also an agronomic crop, so the findings could have direct relevance to crop improvement programs as well as potentially translating into benefits for close relatives including maize, sorghum and sugarcane.

## Supplementary data section

Fig. S1. Field experiment layout for canopy temperature and biomass measurements

## Acknowledgements

Funded by the U.S. Department of Energy under Prime Agreement Nos. DE-SC0008769 and DE-SC0018277. We thank Dr. Timothy Wertin for helping with the stomatal density sample collection and other undergrads and summer interns for their help with field management. We also thank many project partners from the Danforth Plant Science Center, Carnegie Institute,

Washington State University, and University of Minnesota that helped with transplanting seedlings.

# **Author contributions**

A.D.B.L. and I.B. conceived the original research plans. A.D.B.L., P.T.P., D.B., and R.E.P. supervised the experiments. P.T.P. collected the thermal images and processed the images. D.X. collected the stomatal images. P.T.P., D.B., and R.E.P., and L.F. managed the experiment and collected biomass data. P.T.P., M.F., I.B. and A.D.B.L. analyzed and interpreted the data. P.T.P. and A.D.B.L. wrote the article; M.F., I.B., D.B., R.E.P. and L.F. reviewed and commented on the article.

# **References**

**Awika H, Hays D, Mullet J, Rooney W, Weers B.** 2017. QTL mapping and loci dissection for leaf epicuticular wax load and canopy temperature depression and their association with QTL for staygreen in Sorghum bicolor under stress. *Euphytica* **213**, 207.

**Banan D, Paul RE, Feldman MJ, Holmes MW, Schlake H, Baxter I, Jiang H, Leakey ADB.** 2018. High-fidelity detection of crop biomass quantitative trait loci from low-cost imaging in the field. *Plant Direct* **2**, e00041.

**Bates D, Maechler M, Bolker B.** 2015. Walker., S. Fitting linear mixed-effects models using lme4. *Journal of Statistical Software* **67**, 1-48.

**Bennett D, Reynolds M, Mullan D, Izanloo A, Kuchel H, Langridge P, Schnurbusch T.** 2012. Detection of two major grain yield QTL in bread wheat (*Triticum aestivum* L.) under heat, drought and high yield potential environments. *Theoretical and Applied Genetics* **125**, 1473-1485.

**Bennetzen JL, Schmutz J, Wang H, et al.** 2012. Reference genome sequence of the model plant *Setaria*. *Nature Biotechnology* **30**, 555-561.

**Bertolino LT, Caine RS, Gray JE.** 2019. Impact of Stomatal Density and Morphology on Water-Use Efficiency in a Changing World. *Frontiers in Plant Science* **10**, 225.

**Blum A.** 2009. Effective use of water (EUW) and not water-use efficiency (WUE) is the target of crop yield improvement under drought stress. *Field Crops Research* **112**, 119-123.

**Boyer JS.** 1982. Plant productivity and environment. *Science* **218**, 443-448.

467 **Broman KW, Wu H, Sen S, Churchill GA.** 2003. R/qtl: QTL mapping in experimental crosses.  
468 *Bioinformatics* **19**, 889-890.

469 **Brutnell TP, Wang L, Swartwood K, Goldschmidt A, Jackson D, Zhu XG, Kellogg E, Van Eck J.**  
470 2010. *Setaria viridis*: a model for C4 photosynthesis. *Plant Cell* **22**, 2537-2544.

471 **Cattivelli L, Rizza F, Badeck F-W, Mazzucotelli E, Mastrangelo AM, Francia E, Marè C, Tondelli**  
472 **A, Stanca AM.** 2008. Drought tolerance improvement in crop plants: an integrated view from  
473 breeding to genomics. *Field Crops Research* **105**, 1-14.

474 **Condon AG, Richards RA, Rebetzke GJ, Farquhar GD.** 2002. Improving Intrinsic Water-Use  
475 Efficiency and Crop Yield. *Crop Science* **42**, 122-131.

476 **Condon AG, Richards RA, Rebetzke GJ, Farquhar GD.** 2004. Breeding for high water-use  
477 efficiency. *Journal of Experimental Botany* **55**, 2447-2460.

478 **Deery DM, Rebetzke G, Jimenez-Berni JA, Bovill B, James RA, Condon AG, Furbank R,**  
479 **Chapman S, Fischer R.** 2019. Evaluation of the phenotypic repeatability of canopy temperature  
480 in wheat using continuous-terrestrial and airborne measurements. *Frontiers in Plant Science* **10**,  
481 875.

482 **Deery DM, Rebetzke GJ, Jimenez-Berni JA, James RA, Condon AG, Bovill WD, Hutchinson P,**  
483 **Scarrow J, Davy R, Furbank RT.** 2016. Methodology for high-throughput field phenotyping of  
484 canopy temperature using airborne thermography. *Frontiers in Plant Science* **7**, 1808.

485 **Delgado D, Sánchez-Bermejo E, De Marcos A, Martín-Jimenez C, Fenoll C, Alonso-Blanco C,**  
486 **Mena M.** 2019. A genetic dissection of natural variation for stomatal abundance traits in  
487 *Arabidopsis*. *Frontiers in Plant Science* **10**, 1392.

488 **Des Marais DL, Hernandez KM, Juenger TE.** 2013. Genotype-by-environment interaction and  
489 plasticity: exploring genomic responses of plants to the abiotic environment. *Annual Review of*  
490 *Ecology, Evolution, and Systematics* **44**, 5-29.

491 **Devos KM, Wang Z, Beales J, Sasaki T, Gale M.** 1998. Comparative genetic maps of foxtail millet  
492 (*Setaria italica*) and rice (*Oryza sativa*). *Theoretical and Applied Genetics* **96**, 63-68.

493 **Dillen SY, Marron N, Koch B, Ceulemans R.** 2008. Genetic variation of stomatal traits and  
494 carbon isotope discrimination in two hybrid poplar families (*Populus deltoides* 'S9-2' × *P. nigra*  
495 'Ghoy' and *P. deltoides* 'S9-2' × *P. trichocarpa* 'V24'). *Annals of Botany* **102**, 399-407.

496 **Dittberner H, Korte A, Mettler-Altmann T, Weber AP, Monroe G, de Meaux J.** 2018. Natural  
497 variation in stomata size contributes to the local adaptation of water-use efficiency in  
498 *Arabidopsis thaliana*. *Molecular Ecology* **27**, 4052-4065.

499 **Dow GJ, Bergmann DC.** 2014. Patterning and processes: how stomatal development defines  
500 physiological potential. *Current Opinion in Plant Biology* **21**, 67-74.

501 **Ellsworth PZ, Feldman MJ, Baxter I, Cousins AB.** 2020. A genetic link between leaf carbon  
502 isotope composition and whole-plant water use efficiency in the C4 grass *Setaria*. *The Plant*  
503 *Journal* **102**, 1234–1248.

504 **Faralli M, Matthews J, Lawson T.** 2019. Exploiting natural variation and genetic manipulation of  
505 stomatal conductance for crop improvement. *Current Opinion in Plant Biology* **49**, 1-7.

506 **Farquhar G, Hubick K, Condon A, Richards R.** 1989. Carbon isotope fractionation and plant  
507 water-use efficiency. *Stable isotopes in ecological research*: Springer, 21-40.

508 **Feldman MJ, Ellsworth PZ, Fahlgren N, Gehan MA, Cousins AB, Baxter I.** 2018. Components of  
509 water use efficiency have unique genetic signatures in the model C4 grass *Setaria*. *Plant*  
510 *Physiology* **178**, 699-715.

511 **Feldman MJ, Paul RE, Banan D, et al.** 2017. Time dependent genetic analysis links field and  
512 controlled environment phenotypes in the model C4 grass *Setaria*. *PLoS Genetics* **13**, e1006841.

513 **Fetter KC, Eberhardt S, Barclay RS, Wing S, Keller SR.** 2019. StomataCounter: a neural network  
514 for automatic stomata identification and counting. *New Phytologist* **223**, 1671-1681.

515 **Fischer R, Rees D, Sayre K, Lu Z-M, Condon A, Saavedra AL.** 1998. Wheat yield progress  
516 associated with higher stomatal conductance and photosynthetic rate, and cooler canopies.  
517 *Crop science* **38**, 1467-1475.

518 **Gailing O, LANGENFELD-HEYSER R, Polle A, Finkeldey R.** 2008. Quantitative trait loci affecting  
519 stomatal density and growth in a *Quercus robur* progeny: implications for the adaptation to  
520 changing environments. *Global Change Biology* **14**, 1934-1946.

521 **Gray SB, Dermody O, Klein SP, et al.** 2016. Intensifying drought eliminates the expected  
522 benefits of elevated carbon dioxide for soybean. *Nature Plants* **2**, 16132.

523 **Hall N, Griffiths H, Corlett J, Jones H, Lynn J, King G.** 2005. Relationships between water-use  
524 traits and photosynthesis in *Brassica oleracea* resolved by quantitative genetic analysis. *Plant*  
525 *Breeding* **124**, 557-564.

526 **Hamdy A, Ragab R, Scarascia-Mugnozza E.** 2003. Coping with water scarcity: water saving and  
527 increasing water productivity. *Irrigation and Drainage* **52**, 3-20.

528 **Haus MJ, Kelsch RD, Jacobs TW.** 2015. Application of Optical Topometry to Analysis of the Plant  
529 Epidermis. *Plant Physiology* **169**, 946-959.

530 **Hetherington AM, Woodward FI.** 2003. The role of stomata in sensing and driving  
531 environmental change. *Nature* **424**, 901-908.

532 **Jones HG.** 2004. Application of thermal imaging and infrared sensing in plant physiology and  
533 ecophysiology. *Advances in Botanical Research*, Vol. 41: Elsevier, 107-163.

534 **Khazaei H, O'Sullivan DM, Sillanpää MJ, Stoddard FL.** 2014. Use of synteny to identify  
535 candidate genes underlying QTL controlling stomatal traits in faba bean (*Vicia faba* L.).  
536 *Theoretical and Applied Genetics* **127**, 2371-2385.

537 **Khazaie H, Mohammady S, Monneveux P, Stoddard F.** 2011. The determination of direct and  
538 indirect effects of carbon isotope discrimination ( $\Delta$ ), stomatal characteristics and water use  
539 efficiency on grain yield in wheat using sequential path analysis. *Australian Journal of Crop*  
540 *Science* **5**, 466.

541 **Kholová J, Hash CT, Kakker A, Kočová M, Vadez V.** 2010. Constitutive water-conserving  
542 mechanisms are correlated with the terminal drought tolerance of pearl millet [*Pennisetum*  
543 *glaucum* (L.) R. Br.]. *Journal of Experimental Botany* **61**, 369-377.

544 **Kulya C, Siangliwb JL, Toojindab T, Lontoma W, Pattanagula W, Sriyota N, Sanitchon J,**  
545 **Theerakulpisuta P.** 2018. Variation in leaf anatomical characteristics in chromosomal segment  
546 substitution lines of KDML105 carrying drought tolerant QTL segments. *ScienceAsia* **44**, 197-  
547 211.

548 **Kwak I-Y, Moore CR, Spalding EP, Broman KW.** 2014. A simple regression-based method to  
549 map quantitative trait loci underlying function-valued phenotypes. *Genetics* **197**, 1409-1416.

550 **Laza MRC, Kondo M, Ideta O, Barlaan E, Imbe T.** 2010. Quantitative trait loci for stomatal  
551 density and size in lowland rice. *Euphytica* **172**, 149-158.

552 **Leakey AD, Ferguson JN, Pignion CP, Wu A, Jin Z, Hammer GL, Lobell DB.** 2019. Water use  
553 efficiency as a constraint and target for improving the resilience and productivity of C3 and C4  
554 crops. *Annual Review of Plant Biology* **70**, 781-808.

555 **Li K, Huang J, Song W, Wang J, Lv S, Wang X.** 2019. Automatic segmentation and measurement  
556 methods of living stomata of plants based on the CV model. *Plant methods* **15**, 67.

557 **Li P, Brutnell TP.** 2011. *Setaria viridis* and *Setaria italica*, model genetic systems for the Panicoid  
558 grasses. *Journal of Experimental Botany* **62**, 3031-3037.

559 **Liu X, Fan Y, Mak M, et al.** 2017. QTLs for stomatal and photosynthetic traits related to salinity  
560 tolerance in barley. *BMC Genomics* **18**, 9.

561 **Liu Y, Subhash C, Yan J, Song C, Zhao J, Li J.** 2011. Maize leaf temperature responses to  
562 drought: Thermal imaging and quantitative trait loci (QTL) mapping. *Environmental and*  
563 *Experimental Botany* **71**, 158-165.

564 **Lu J, He J, Zhou X, Zhong J, Li J, Liang Y-K.** 2019. Homologous genes of epidermal patterning  
565 factor regulate stomatal development in rice. *Journal of Plant Physiology* **234**, 18-27.

566 **Martre P, Cochard H, Durand JL.** 2001. Hydraulic architecture and water flow in growing grass  
567 tillers (*Festuca arundinacea* Schreb.). *Plant, Cell & Environment* **24**, 65-76.

568 **Mason RE, Hays DB, Mondal S, Ibrahim AM, Basnet BR.** 2013. QTL for yield, yield components  
569 and canopy temperature depression in wheat under late sown field conditions. *Euphytica* **194**,  
570 243-259.

571 **Mauro-Herrera M, Doust AN.** 2016. Development and Genetic Control of Plant Architecture  
572 and Biomass in the Panicoid Grass, *Setaria*. *PLoS One* **11**, e0151346.

573 **Mohammed U, Caine R, Atkinson J, Harrison E, Wells D, Chater C, Gray J, Swarup R, Murchie**  
574 **E.** 2019. Rice plants overexpressing OsEPF1 show reduced stomatal density and increased root  
575 cortical aerenchyma formation. *Scientific reports* **9**, 1-13.

576 **Morison J, Baker N, Mullineaux P, Davies W.** 2007. Improving water use in crop production.  
577 *Philosophical Transactions of the Royal Society B: Biological Sciences* **363**, 639-658.

578 **Nakashima K, Takasaki H, Mizoi J, Shinozaki K, Yamaguchi-Shinozaki K.** 2012. NAC  
579 transcription factors in plant abiotic stress responses. *Biochimica et Biophysica Acta (BBA)-Gene*  
580 *Regulatory Mechanisms* **1819**, 97-103.

581 **Nelson DE, Repetti PP, Adams TR, Creelman RA, Wu J, Warner DC, Anstrom DC, Bensen RJ,**  
582 **Castiglioni PP, Donnarummo MG.** 2007. Plant nuclear factor Y (NF-Y) B subunits confer drought  
583 tolerance and lead to improved corn yields on water-limited acres. *Proceedings of the National*  
584 *Academy of Sciences* **104**, 16450-16455.

585 **Nemali KS, Bonin C, Dohleman FG, Stephens M, Reeves WR, Nelson DE, Castiglioni P, Whitsel**  
586 **JE, Sammons B, Silady RA.** 2015. Physiological responses related to increased grain yield under  
587 drought in the first biotechnology-derived drought-tolerant maize. *Plant, Cell & Environment*  
588 **38**, 1866-1880.

589 **Nunes TD, Zhang D, Raissig MT.** 2020. Form, development and function of grass stomata. *The*  
590 *Plant Journal* **101**, 780-799.

591 **Ohsumi A, Kanemura T, Homma K, Horie T, Shiraiwa T.** 2007. Genotypic variation of stomatal  
592 conductance in relation to stomatal density and length in rice (*Oryza sativa* L.). *Plant Production*  
593 *Science* **10**, 322-328.

594 **Prado SA, Cabrera-Bosquet L, Grau A, Coupel-Ledru A, Millet EJ, Welcker C, Tardieu F.** 2018.  
595 Phenomics allows identification of genomic regions affecting maize stomatal conductance with  
596 conditional effects of water deficit and evaporative demand. *Plant, Cell & Environment* **41**, 314-  
597 326.

598 **Raissig MT, Matos JL, Gil MXA, Kornfeld A, Bettadapur A, Abrash E, Allison HR, Badgley G,**  
599 **Vogel JP, Berry JA.** 2017. Mobile MUTE specifies subsidiary cells to build physiologically  
600 improved grass stomata. *Science* **355**, 1215-1218.

601 **Rowland-Bamford AJ, Nordenbrock C, Baker JT, Bowes G, Allen Jr LH.** 1990. Changes in  
602 stomatal density in rice grown under various CO<sub>2</sub> regimes with natural solar irradiance.  
603 *Environmental and Experimental Botany* **30**, 175-180.

604 **Sagan V, Maimaitijiang M, Sidike P, Eblimit K, Peterson KT, Hartling S, Esposito F, Khanal K,**  
605 **Newcomb M, Pauli D.** 2019. UAV-based high resolution thermal imaging for vegetation  
606 monitoring, and plant phenotyping using ICI 8640 P, FLIR Vue Pro R 640, and thermomap  
607 cameras. *Remote Sensing* **11**, 330.

608 **Schoppach R, Taylor JD, Majerus E, Claverie E, Baumann U, Suchecki R, Fleury D, Sadok W.**  
609 2016. High resolution mapping of traits related to whole-plant transpiration under increasing  
610 evaporative demand in wheat. *Journal of Experimental Botany* **67**, 2847-2860.

611 **Shahinnia F, Le Roy J, Laborde B, Sznajder B, Kalambettu P, Mahjourimajd S, Tilbrook J, Fleury**  
612 **D.** 2016. Genetic association of stomatal traits and yield in wheat grown in low rainfall  
613 environments. *BMC Plant Biology* **16**, 150.

614 **Sinclair TR, Devi J, Shekoofa A, Choudhary S, Sadok W, Vadez V, Riar M, Rufty T.** 2017.  
615 Limited-transpiration response to high vapor pressure deficit in crop species. *Plant Science* **260**,  
616 109-118.

617 **Stocker TF, Qin D, Plattner G-K, Tignor M, Allen SK, Boschung J, Nauels A, Xia Y, Bex V,**  
618 **Midgley PM.** 2013. *Climate change 2013: The physical science basis.* Cambridge University Press  
619 Cambridge.

620 **Tardieu F.** 2013. Plant response to environmental conditions: assessing potential production,  
621 water demand, and negative effects of water deficit. *Frontiers in Physiology* **4**, 17.

622 **Turner NC, Wright GC, Siddique K.** 2001. Adaptation of grain legumes (pulses) to water-limited  
623 environments. *Advances in Agronomy*  
624 **71**, 193-231.

625 **Valliyodan B, Nguyen HT.** 2006. Understanding regulatory networks and engineering for  
626 enhanced drought tolerance in plants. *Current Opinion in Plant Biology* **9**, 189-195.

627 **Violet-Chabrand S, Lawson T.** 2019. Dynamic leaf energy balance: deriving stomatal  
628 conductance from thermal imaging in a dynamic environment. *Journal of Experimental Botany*  
629 **70**, 2839-2855.

630 **Wang SG, Jia SS, Sun DZ, Hua F, Chang XP, Jing RL.** 2016. Mapping QTLs for stomatal density  
631 and size under drought stress in wheat (*Triticum aestivum* L.). *Journal of Integrative Agriculture*  
632 **15**, 1955-1967.

633 **Wang Z, Devos K, Liu C, Wang R, Gale M.** 1998. Construction of RFLP-based maps of foxtail  
634 millet, *Setaria italica* (L.) P. Beauv. *Theoretical and Applied Genetics* **96**, 31-36.

- White T, Snow V.** 2012. A modelling analysis to identify plant traits for enhanced water-use efficiency of pasture. *Crop and Pasture Science* **63**, 63-76.
- Xu Z, Zhou G.** 2008. Responses of leaf stomatal density to water status and its relationship with photosynthesis in a grass. *Journal of Experimental Botany* **59**, 3317-3325.
- Zhang JZ, Creelman RA, Zhu J-K.** 2004. From laboratory to field. Using information from *Arabidopsis* to engineer salt, cold, and drought tolerance in crops. *Plant physiology* **135**, 615-621.

Table 1. Regression parameters for total above-ground biomass (g per plant) in relation to canopy temperature (°C) and stomatal density (pores per mm<sup>2</sup>) of Setaria genotypes grown under wet and dry treatments.

Biomass = Intercept (b) + a(Canopy temperature)

			Intercept (b)	Slope (a)	R <sup>2</sup>	p-value
Canopy temperature	30 DAS	Wet	40.00	-1.19	0.13	< 0.001
		Dry	24.02	-0.63	0.09	< 0.001
	32 DAS	Wet	58.21	-1.82	0.24	< 0.001
		Dry	27.01	-0.74	0.20	< 0.001

Biomass = Intercept (b) + a(Stomatal density)

Stomatal density	Wet	8.94	-0.05	0.05	0.012
	Dry	8.31	-0.06	0.10	< 0.001

Table 2. Putative quantitative trait loci (QTLs) for stomatal density and canopy temperature traits in the 120 F<sub>7</sub> recombinant inbred line population derived from a cross of *S.italica* and *S.viridis*, and B100 parental line.

Trait	Peak marker	Chr	Pos (cM) <sup>1</sup>	LOD at Peak <sup>2</sup>	Variance (%) <sup>3</sup>	Additive effect	Left CI (cM) <sup>4</sup>	Right CI (cM)
SD	S5_42996052	5	104.8	8.3	20.8	-3.8	101.1	106.6
	S9_10073675	9	45.6	5.0	11.6	-2.3	40.4	52.7
	S9_50690449	9	136.5	3.7	8.3	-2.0	133.0	146.9
CT wet 30 DAS	S5_39309008	5	93.8	4.4	10.0	-0.2	76.2	104.1
	S7_31494503	7	93.3	9.2	23.1	0.3	89.3	101.9
	S9_6724364	9	34.9	8.8	21.8	-0.2	33.9	38.6
CT wet 32 DAS	S7_31494503	7	93.3	3.8	12.0	0.2	89.3	101.9
	S9_6724364	9	34.9	6.4	21.0	-0.2	32.8	38.6
CT dry 30 DAS	S5_39309008	5	93.8	5.7	14.1	-0.2	92.8	100.2
	S7_32133319	7	99.9	8.0	21.1	0.4	92.5	101.9
	S9_7218054	9	35.9	6.0	15.0	-0.2	32.8	38.6

<sup>1</sup>Position of the peak marker in centimorgan (cM); <sup>2</sup> Logarithm of odds (LOD) of the peak marker, <sup>3</sup> Percentage of phenotypic variance explained by the QTL, <sup>4</sup> Left confidence interval of the QTL.

Fig. 1. Daily average values of air temperature (a) and relative humidity (b) at SoyFACE experimental field site. The horizontal dotted line indicates the mean over the entire growing season. The vertical dashed lines indicate the days after sowing the canopy temperature measurements were collected in the field.

Fig. 2. Aerial infra-red and RGB images of *Setaria* subplots under awnings in wet and dry treatments. Infra-red image of wet awning (a) and dry awning (b). RGB image of wet awning (c) and dry awning (d). The square boxes are the measured area of each subplot canopy.

Fig. 3. Soil volumetric water content (% vol/vol) at depths of 5 cm and 25 cm over the growing season in plots of *Setaria* supplied with either regular irrigation to maintain adequate water supply (wet treatment; light grey) or receiving no irrigation (dry treatment; dark grey). Rainfall was blocked from entering plots of both treatments using retractable rainout shelters. Data points and error bars shown the mean and standard error of three replicates per treatment. The dashed vertical lines indicate the dates when canopy temperature was measured.

Fig. 4. Frequency distribution of stomatal density (pores mm<sup>-2</sup>) of 120 recombinant inbred lines derived from a cross of *S. italica* and *S. viridis*, and B100 parental line. Data are genotype means derived from two fields of view per leaf from each of four replicate plants. The dotted vertical lines represent the population mean value.

Fig. 5. Stomatal density of 120 recombinant inbred lines derived from a cross of *S.italica* and *S.viridis*, and B100 parental line. Bars represent the genotype means ( $\pm$  standard error, n=4) derived from two fields of view from each of four replicate plants.

Fig. 6. Frequency distribution of canopy temperature (°C) of 120 RILs in wet (light grey) and dry (dark grey) treatments at 30 and 32 days after sowing (DAS). Data are means derived from all pixels in the interior of three replicate plots per genotype. The dashed vertical lines represent the treatment mean value for each treatment.

Fig. 7. Scatterplot of midday canopy temperature for Setaria RILs and B100 on 30 DAS versus 32 DAS under wet (●) and dry treatments (●). Lines of best fit are shown along with the Pearson's correlation coefficient (r) and associated p-value.

Fig. 8. Scatterplot of total biomass (g per plant) in relation to canopy temperature (°C) for Setaria RILs and the parent lines (A10 and B100) under wet (●) and dry conditions (●) at 30 and 32 days after sowing (DAS). Data are best linear unbiased predicted (BLUP) values for each genotype. Lines of best fit are shown along with the Pearson's correlation coefficient (r) and associated p-value.

Fig. 9. Scatterplot of canopy temperature (°C) in relation to stomatal density (pores mm<sup>-2</sup>) for Setaria RILs and the parent lines (A10 and B100) under wet (●) and dry (●) conditions at 30 and 32 days after sowing (DAS). Data are best linear unbiased predicted (BLUP) values for each genotype. Lines of best fit are shown along with the Pearson's correlation coefficient (r) and associated p-value.

Fig. 10. Scatterplot of total biomass (g per plant) relative to stomatal density (pores mm<sup>-2</sup>) for Setaria RILs and the parent lines (A10 and B100) under wet (●) and dry (●) conditions. Data are best linear unbiased predicted (BLUP) values for each genotype. Lines of best fit are shown along with the Pearson's correlation coefficient (r) and associated p-value.

Fig. 11. QTLs identified for stomatal density (SD) and canopy temperature (CT) under wet (grey) and dry (pink) treatments in the Setaria RIL population. Each panel corresponds to a chromosome. The arrow marks indicate the direction of the B100 allelic effect.

Fig. 12. QTLs on chromosomes 5, 7 and 9 identified across multiple studies of *S. italica* x *S. viridis* RIL population (Mauro-Herrera and Doust, 2016; Feldman et al., 2017; Banan et al., 2018;

Feldman et al., 2018; Ellsworth et al., 2019). The arrow marks indicate the direction of the B100 allelic effect. The QTLs for stomatal density and canopy temperature identified in this study are denoted in bold and italics. BN – Branch number, CH – Culm height, CT – Canopy temperature, D13C – Delta13C, LM – Leaf mass, ML – Mesocotyl length, PAI – Plant area index, PE – Panicle emergence, PH – Plant height, PM – Panicle mass, RVR – Reproductive to vegetative mass ratio, SD – Stomatal density, STH – Secondary tiller height, VM – Vegetative mass, WUE – Water-use efficiency.

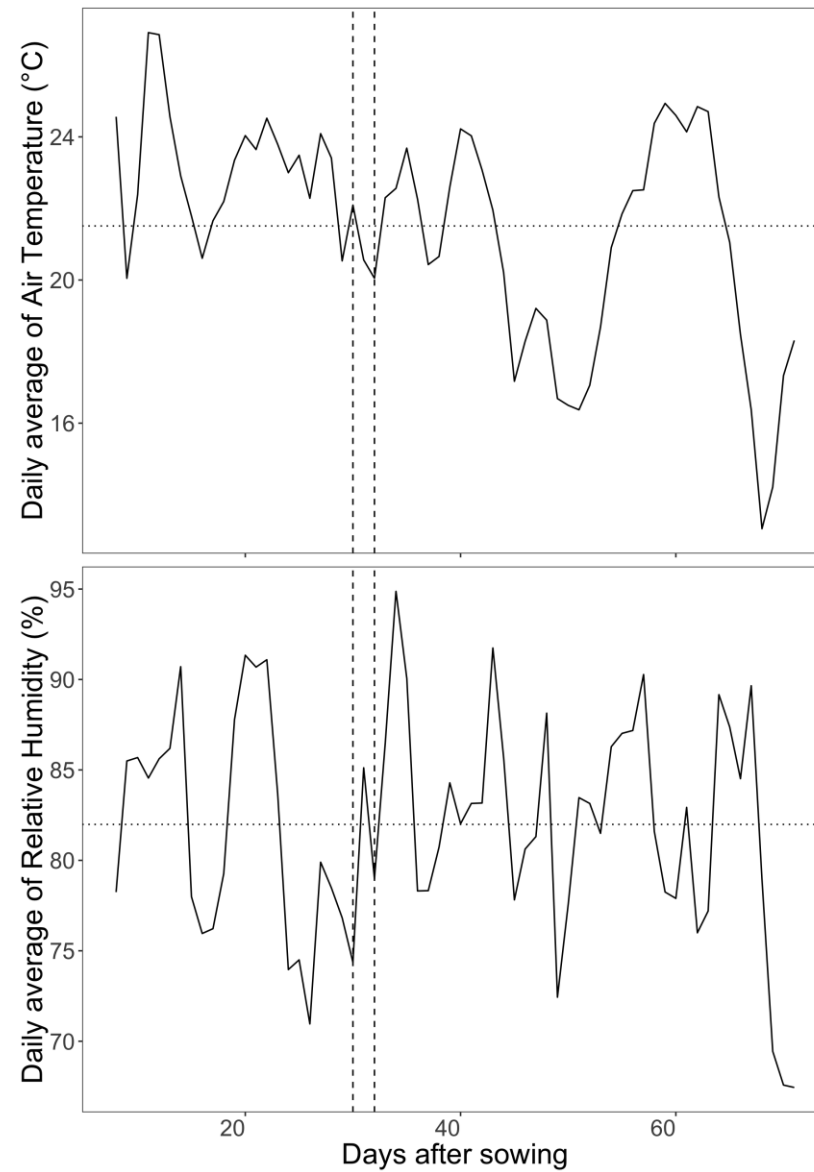


Fig. 1. Daily average values of air temperature (a) and relative humidity (b) at SoyFACE experimental field site. The horizontal dotted line indicates the mean over the entire growing season. The vertical dashed lines indicate the days after sowing the canopy temperature measurements were collected in the field.

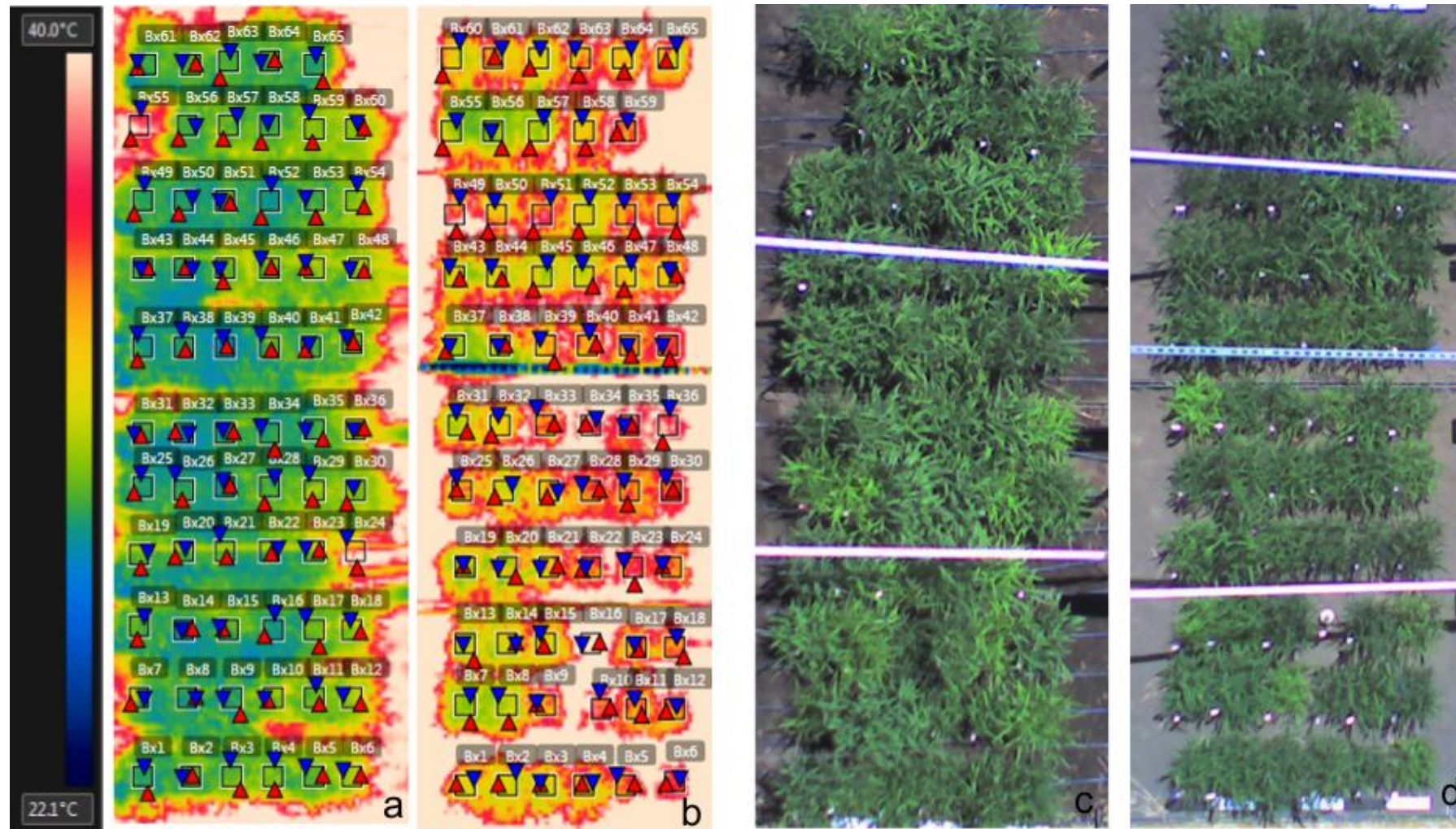


Fig. 2. Aerial infra-red and RGB images of *Setaria* subplots under awnings in wet and dry treatments. Infra-red image of wet awning (a) and dry awning (b). RGB image of wet awning (c) and dry awning (d). The square boxes are the measured area of each subplot canopy.

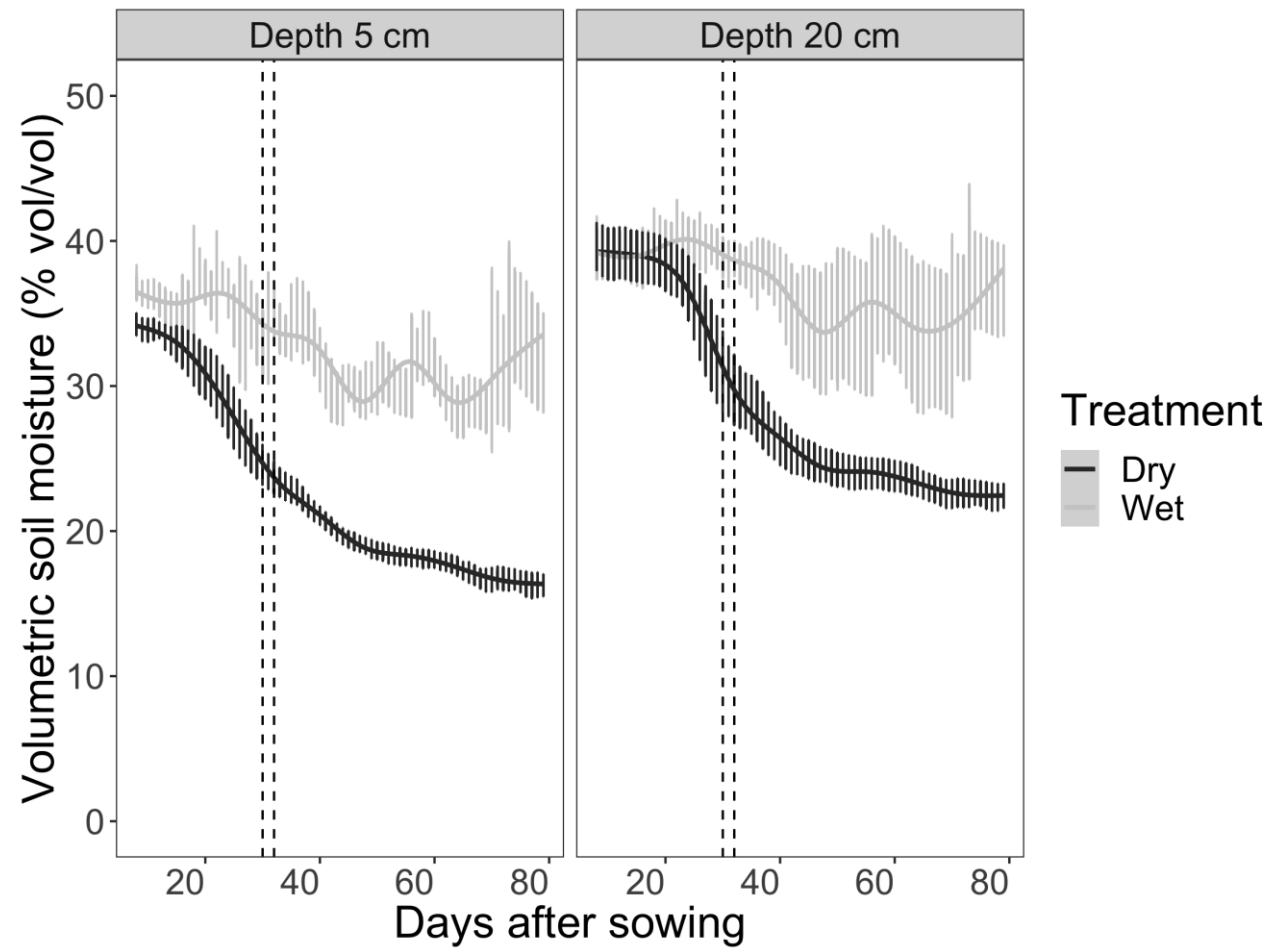


Fig. 3. Soil volumetric water content (% vol/vol) at depths of 5 cm and 25 cm over the growing season in plots of *Setaria* supplied with either regular irrigation to maintain adequate water supply (wet treatment; light grey) or receiving no irrigation (dry treatment; dark grey). Rainfall was blocked from entering plots of both treatments using retractable rainout shelters. Data points and error bars shown the mean and standard error of three replicates per treatment. The dashed vertical lines indicate the dates when canopy temperature was measured.

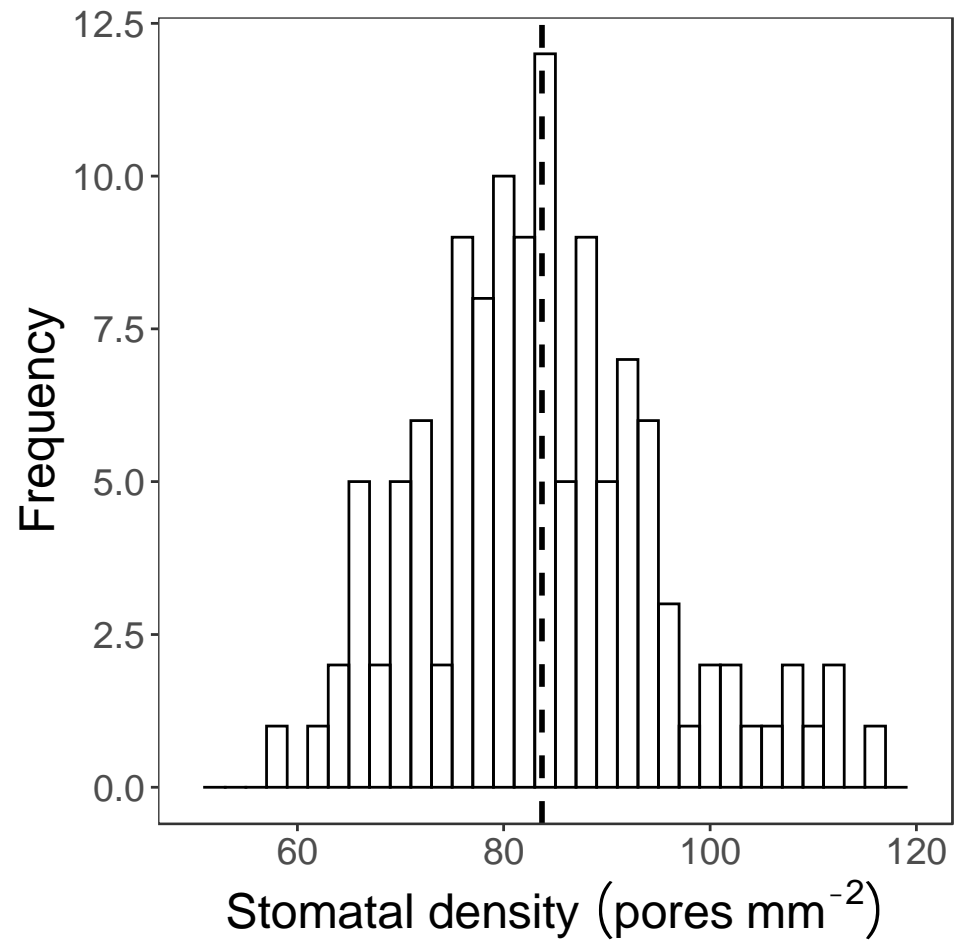


Fig. 4. Frequency distribution of stomatal density (pores mm<sup>-2</sup>) of 120 recombinant inbred lines derived from a cross of *S. italica* and *S. viridis*, and B100 parental line. Data are genotype means derived from two fields of view per leaf from each of four replicate plants. The dotted vertical lines represent the population mean value.

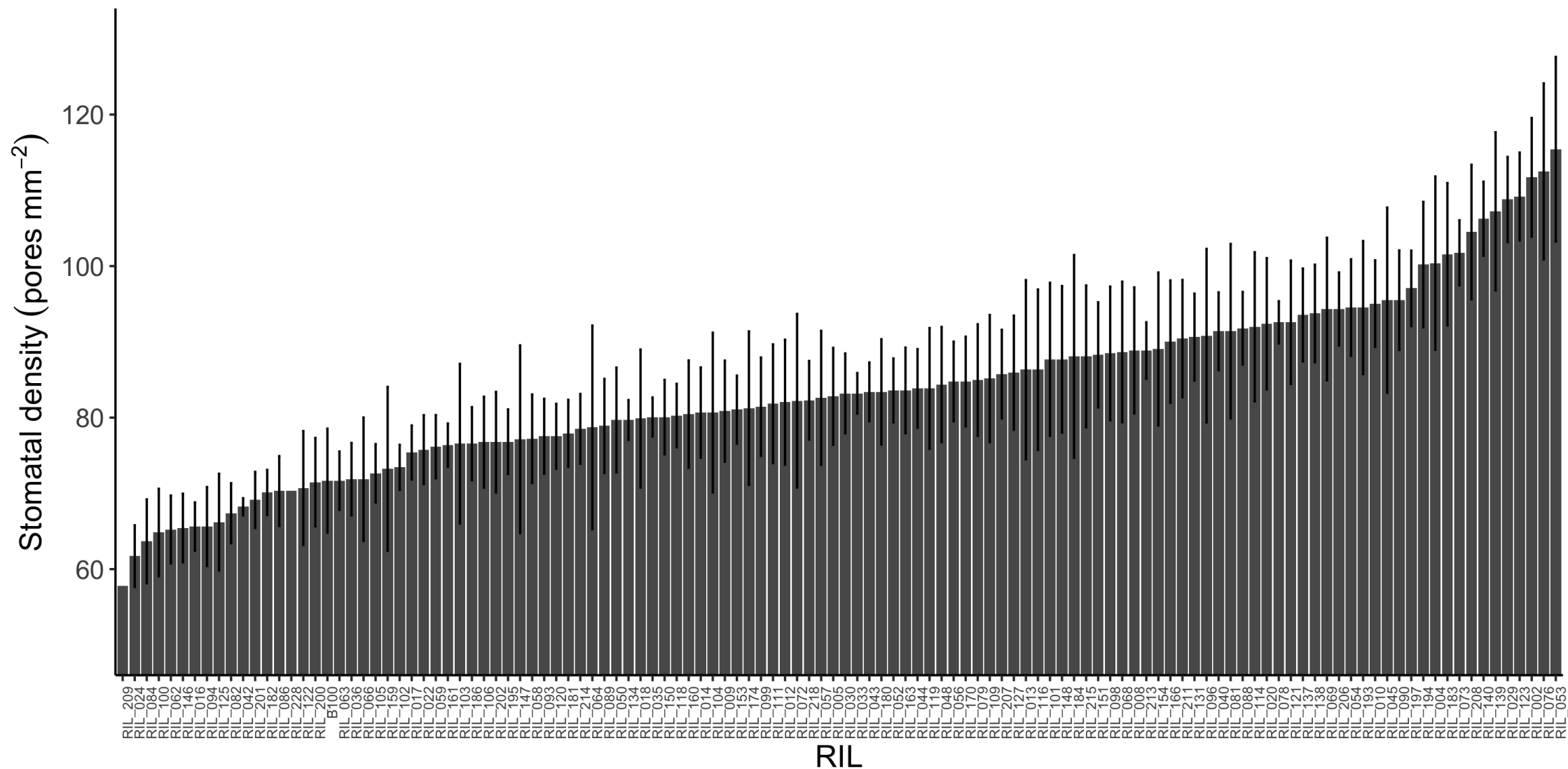


Fig. 5. Stomatal density of 120 recombinant inbred lines derived from a cross of *S.italica* and *S.viridis*, and B100 parental line. Bars represent the genotype means ( $\pm$  standard error, n=4) derived from two fields of view from each of four replicate plants.

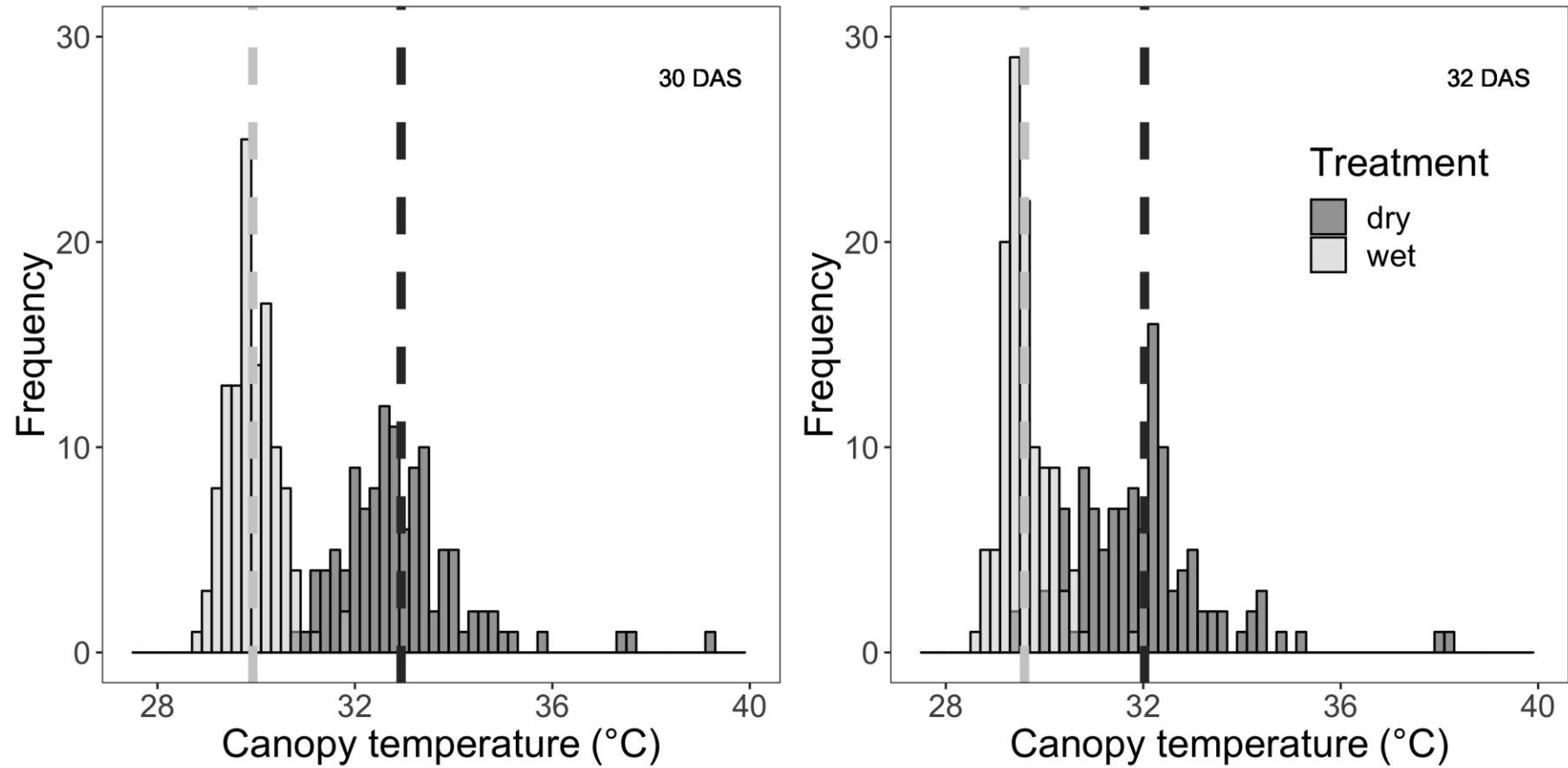


Fig. 6. Frequency distribution of canopy temperature (°C) of 120 RILs in wet (light grey) and dry (dark grey) treatments at 30 and 32 days after sowing (DAS). Data are means derived from all pixels in the interior of three replicate plots per genotype. The dashed vertical lines represent the treatment mean value for each treatment.

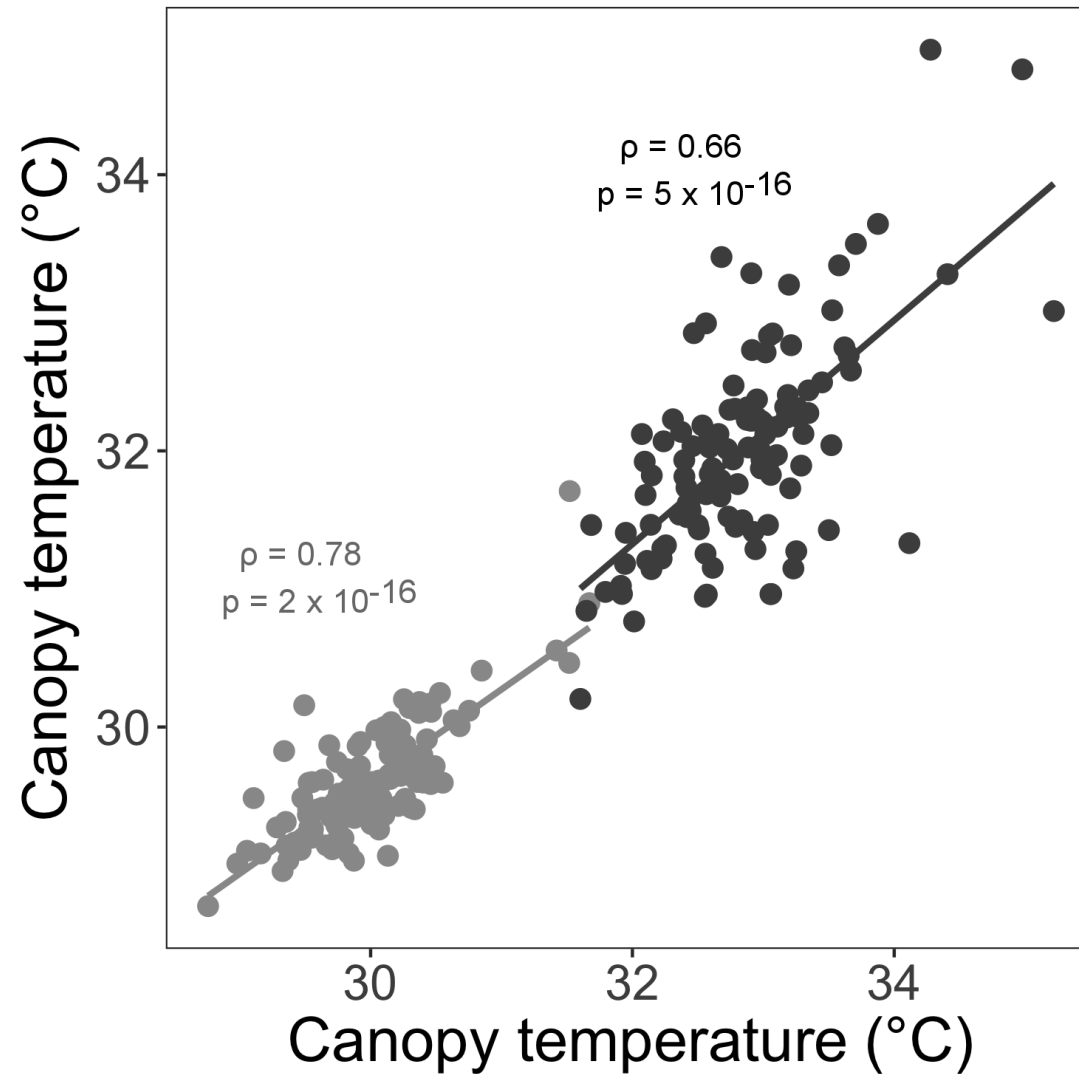


Fig. 7. Scatterplot of midday canopy temperature for Setaria RILs and B100 on 30 DAS versus 32 DAS under wet (●) and dry treatments (●). Lines of best fit are shown along with the Pearson's correlation coefficient ( $r$ ) and associated p-value.

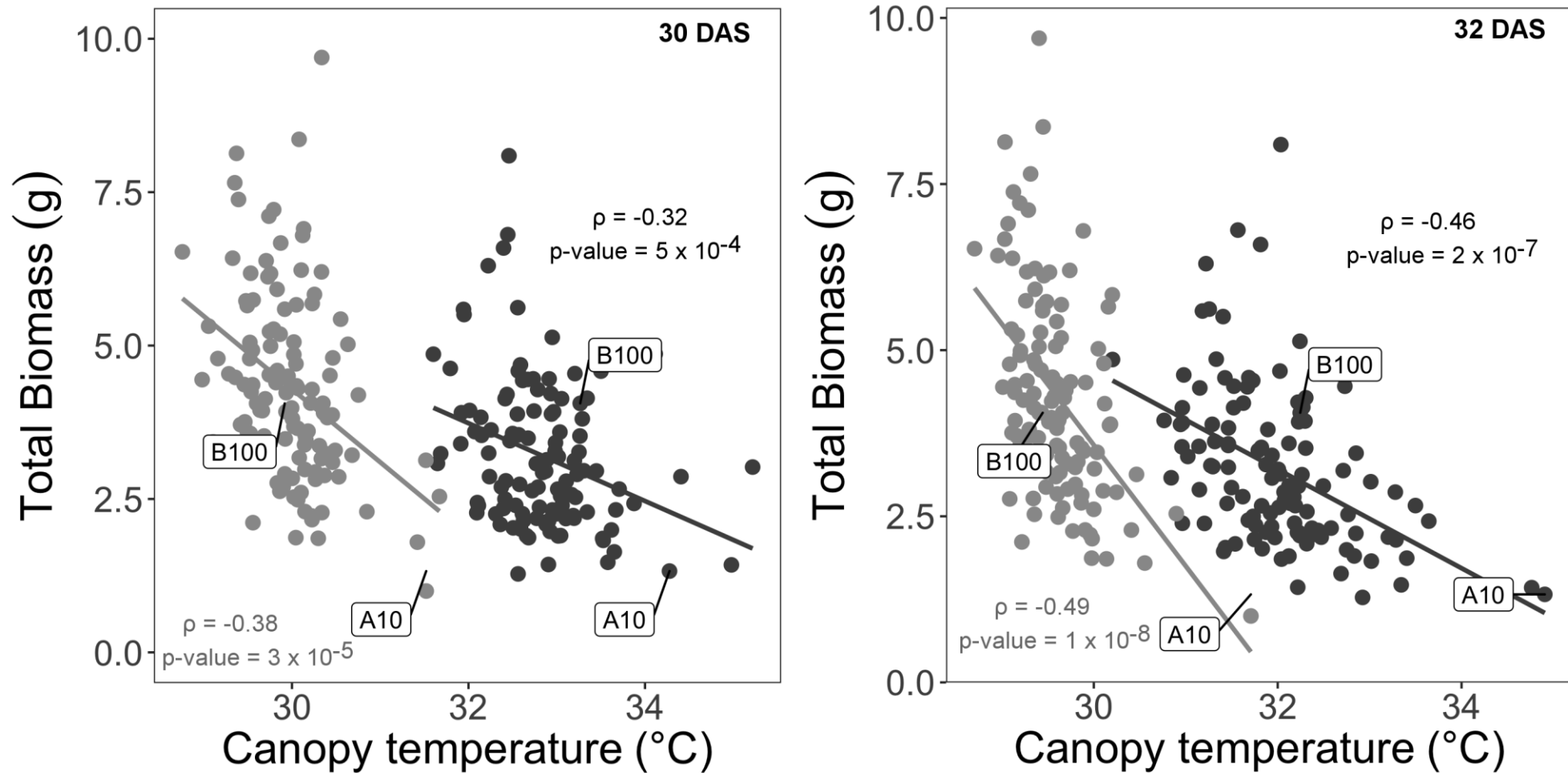


Fig. 8. Scatterplot of total biomass (g per plant) in relation to canopy temperature (°C) for Setaria RILs and the parent lines (A10 and B100) under wet (●) and dry conditions (●) at 30 and 32 days after sowing (DAS). Data are best linear unbiased predicted (BLUP) values for each genotype. Lines of best fit are shown along with the Pearson's correlation coefficient (r) and associated p-value.

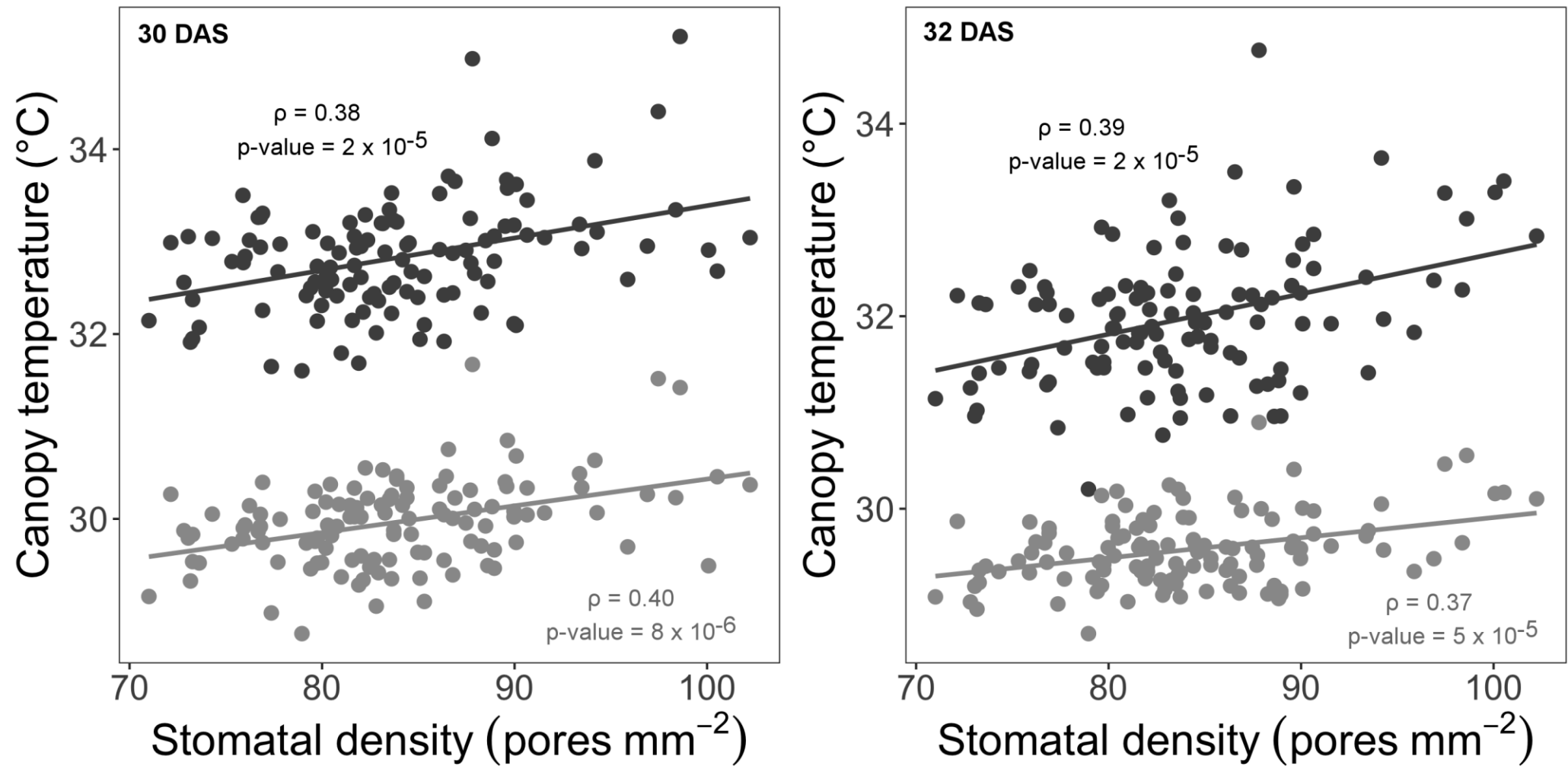


Fig. 9. Scatterplot of canopy temperature (°C) in relation to stomatal density (pores mm<sup>-2</sup>) for Setaria RILs and the parent lines (A10 and B100) under wet (●) and dry (●) conditions at 30 and 32 days after sowing (DAS). Data are best linear unbiased predicted (BLUP) values for each genotype. Lines of best fit are shown along with the Pearson's correlation coefficient (r) and associated p-value.

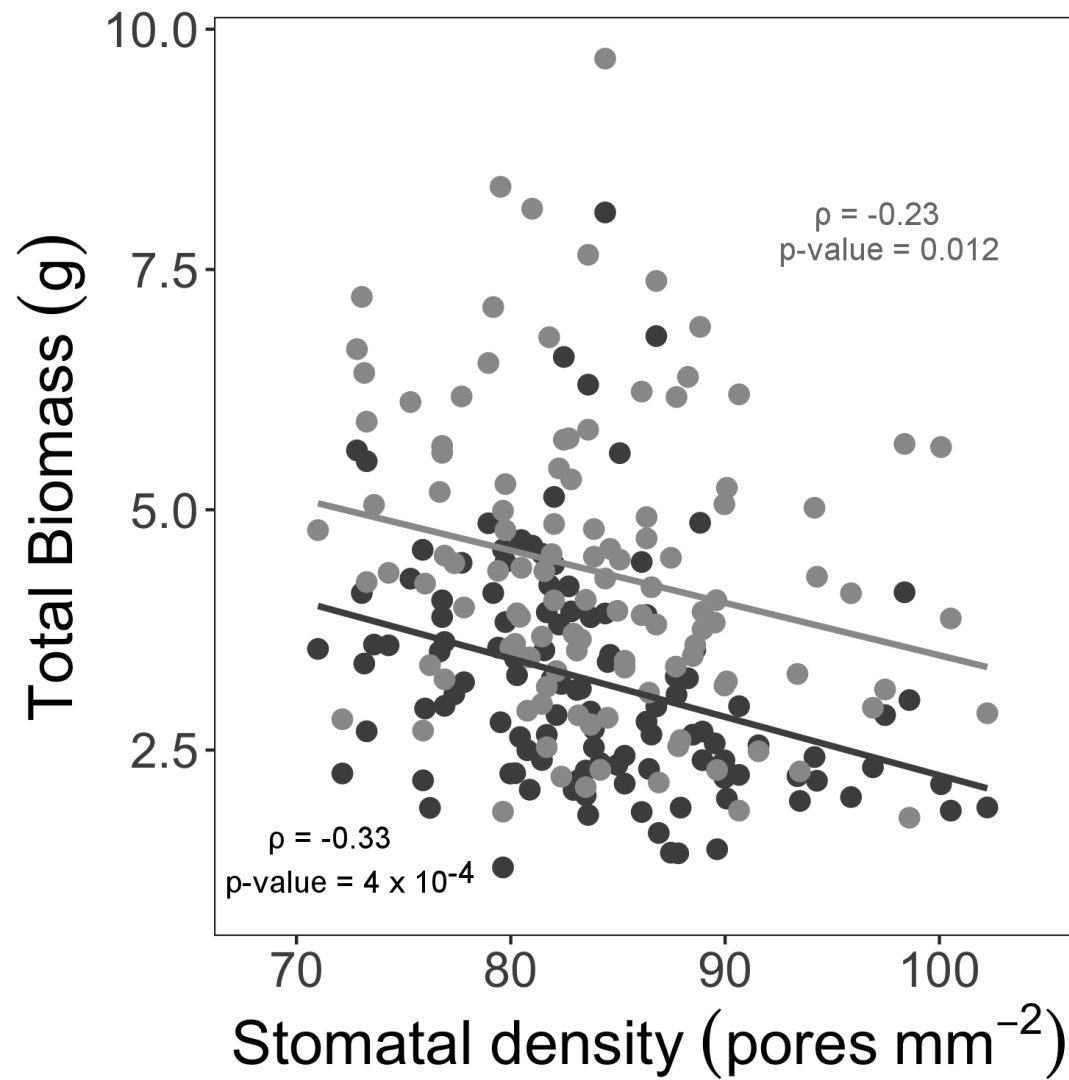


Fig. 10. Scatterplot of total biomass (g per plant) relative to stomatal density (pores mm<sup>-2</sup>) for *Setaria* RILs and the parent lines (A10 and B100) under wet (●) and dry (●) conditions. Data are best linear unbiased predicted (BLUP) values for each genotype. Lines of best fit are shown along with the Pearson's correlation coefficient ( $r$ ) and associated  $p$ -value.

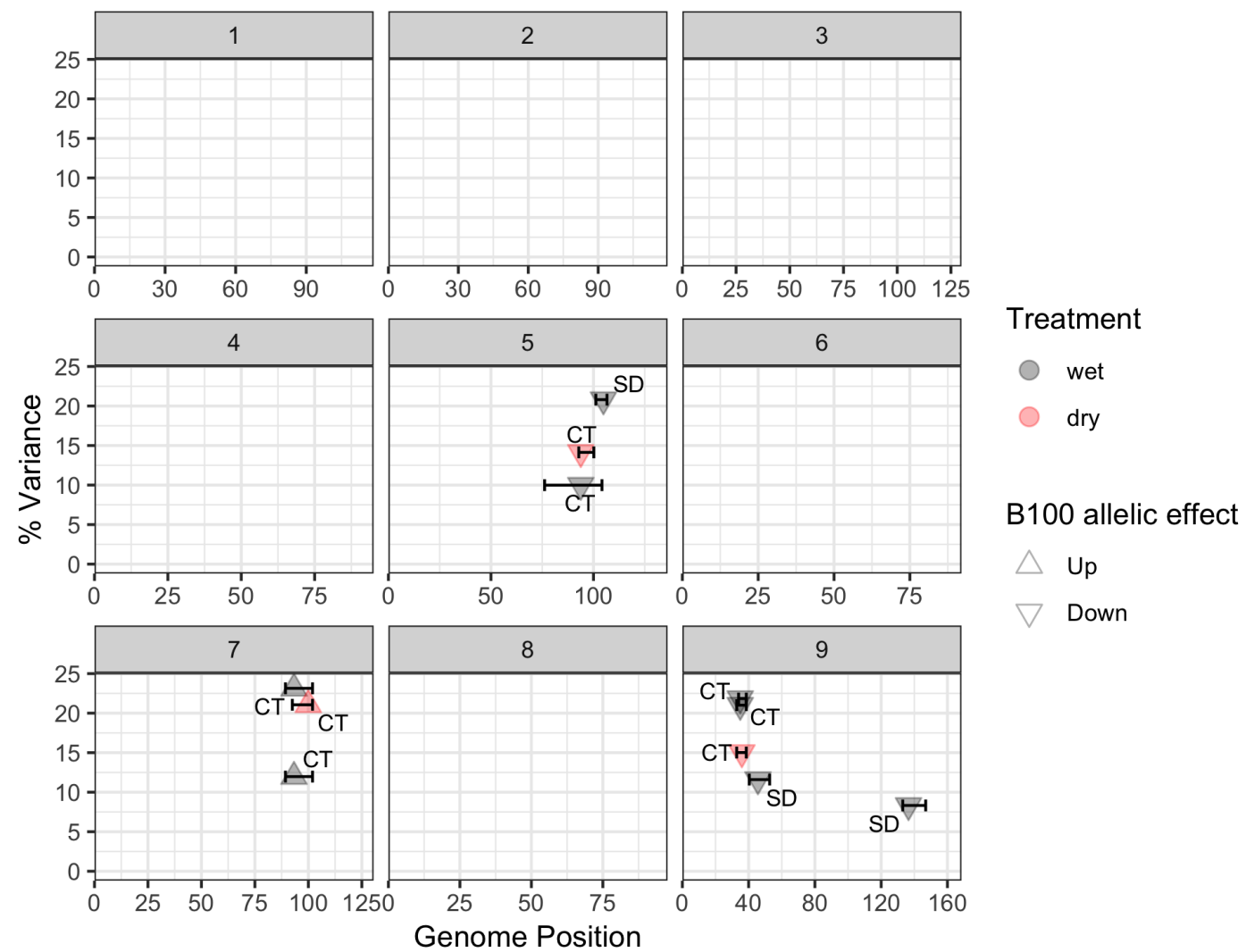


Fig. 11. QTLs identified for stomatal density (SD) and canopy temperature (CT) under wet (grey) and dry (pink) treatments in the Setaria RIL population. Each panel corresponds to a chromosome. The arrow marks indicate the direction of the B100 allelic effect.

